NUCL SCI TECH (2020) 31:61
https://doi.org/10.1007/s41365-020-00766-x

Investigation of the symmetry energy of nuclear matter using isospin-dependent quantum molecular dynamics

Hao Yu[1,2] · **De-Qing Fang**[3,1] · **Yu-Gang Ma**[3,1]

Received: 2 February 2020 / Revised: 2 April 2020 / Accepted: 2 April 2020 / Published online: 30 May 2020

Abstract Simulations of infinite nuclear matter at different densities, isospin asymmetries and temperatures are performed using the isospin-dependent quantum molecular dynamics (IQMD) model to study the equation of state and symmetry energy. A rigorous periodic boundary condition is used in the simulations. Symmetry energies are extracted from the binding energies under different conditions and compared to the classical molecular dynamics (CMD) model using the same method. The results show that both models can reproduce the experimental results for the symmetry energies at low densities, but IQMD is more appropriate than CMD for nuclear matter above the saturation density. This indicates that IQMD may be a reliable model for the study of the properties of infinite nuclear matter.

Keywords Infinite nuclear matter · Symmetry energy · IQMD model

1 Introduction

The nuclear equation of state (EOS) describes the properties of a system with a large number of nucleons. The study this concept is important in both nuclear physics and nuclear astrophysics [1–6]. The nuclear EOS can affect the structure of neutron stars and their evolutionary process. The behavior of symmetric nuclear matter EOS has been well studied both theoretically and experimentally. Moreover, the binding energy of symmetrical nuclear matter near the saturation density (approximately $0.16\ \mathrm{fm}^{-3}$) is known to be -16 MeV. Almost all the nuclear dynamics models, including the classical molecular dynamics (CMD), quantum molecular dynamics (QMD), Boltzmann–Uehling–Uhlenbeck model (BUU), constrained molecular dynamics (CoMD), fermionic molecular dynamics (FMD) and antisymmetrized molecular dynamics (AMD) models, can reliably describe the properties of ideal nuclear matter at the saturation density. QMD provides a good description of the transport process of nuclear collisions in intermediate- and low-energy regions [7–13].

During the past 20 years, studies have also been conducted to simulate nuclear matter via QMD [14, 15]. After the improvement in QMD, the extension of quantum molecular dynamics (EQMD) model was developed [16]. The advantage of this model over QMD is that a phenomenological Pauli potential is introduced into the

This work is partially supported by the National Key R&D Program of China (No. 2018YFA0404404), the National Natural Science Foundation of China (Nos. 11925502, 11935001, 11961141003, 11421505, 11475244 and 11927901), Shanghai Development Foundation for Science and Technology (No. 19ZR1403100), the Strategic Priority Research Program of the CAS (No. XDB34030100 and XDB34030200) and the Key Research Program of Frontier Sciences of the CAS (No. QYZDJ-SSW-SLH002).

✉ De-Qing Fang
dqfang@fudan.edu.cn

Yu-Gang Ma
mayugang@fudan.edu.cn

[1] Shanghai Institute of Applied Physics, Chinese Academy of Sciences, Shanghai 201800, China

[2] University of the Chinese Academy of Sciences, Beijing 100080, China

[3] Key Laboratory of Nuclear Physics and Ion-beam Application (MOE), Institute of Modern Physics, Fudan University, Shanghai 200433, China

effective interactions to approximate the characteristics of a fermion many-body system, and a friction cooling process is added. Compared to QMD, EQMD can simulate the nuclear system in the ground state more reliably. However, the applicable energy region of these two models is different. With these improvements, EQMD can simulate the collective resonance with clusters more reliably near the ground state [17–21]. These different scopes of application render QMD more suitable for simulating a nuclear system at high temperature compared to EQMD. Therefore, the properties of nuclear matter at high temperature can be studied using QMD. In some studies, the CMD model was used to study nuclear matter using the classic potential form and some useful results have been obtained [22, 23]. It will be interesting to compare these results to that obtained using QMD.

The report is organized into several sections. In Sect. 2, we briefly describe the isospin-dependent QMD model, the boundary condition for infinite nuclear matter, as well as the potential parameters. In Sect. 3, we present the binding energies for nuclear matter at different densities, isospin asymmetry, temperature and the extracted symmetry energies. Finally, a summary is presented in Sect. 4.

2 Description of IQMD model

IQMD is the isospin-dependent version of QMD that simulates heavy ion reactions at intermediate energies by individual events. In IQMD, neutrons and protons are distinguished. A nucleon is represented by a Gaussian wave packet of width L,

$$\phi_i(\vec{r}) = \frac{1}{(2\pi L)^{3/4}} \exp\left[-\frac{(\vec{r}-\vec{r}_i(t))^2}{4L} + i\frac{\vec{p}_i(t)\cdot\vec{r}}{\hbar}\right]. \quad (1)$$

In the ith wave packet, r_i represents the position and p_i represents the momentum. The value of L is taken to be 2.16 fm^2, which is the widely used value in most QMD calculations. The direct product of these wave functions is used as the total wave function of the nuclear system. The motion of nucleons in the system follows a regular Hamiltonian relationship,

$$\dot{r}_i = \frac{\partial H}{\partial p_i}, \quad \dot{p}_i = -\frac{\partial H}{\partial r_i}. \quad (2)$$

The distribution function of the nuclear density can be obtained by summing the integral of the Wigner function of the momentum for each nucleon,

$$\rho(\vec{r},t) = \sum_i \frac{1}{(2\pi L)^{3/2}} \exp\left[\frac{-(\vec{r}-\vec{r}_i(t))^2}{2L}\right]. \quad (3)$$

The total potential used in IQMD can usually be expressed as,

$$U = U_{\rm loc}^{(2)} + U_{\rm loc}^{(3)} + U_{\rm Coul} + U_{\rm md} + U_{\rm sym} + U_{\rm surf}, \quad (4)$$

where $U_{\rm loc}^{(2)}$, $U_{\rm loc}^{(3)}$, $U_{\rm Coul}$, $U_{\rm md}$, $U_{\rm sym}$ and $U_{\rm surf}$ are two-body, three-body, Coulomb, momentum-dependent, symmetry and surface potentials, respectively. For infinite nuclear matter studies, the Coulomb and surface potentials are not considered in the present work. The two-body potential and three-body potential are of the Skyrme form,

$$U_{\rm loc}^{(2)} = \frac{\alpha}{2}\frac{\langle\rho\rangle}{\rho_0}, \quad U_{\rm loc}^{(3)} = \frac{\beta}{1+\gamma}\frac{\langle\rho\rangle^\gamma}{\rho_0^\gamma}. \quad (5)$$

EOS with different compression coefficients can be obtained by appropriately adjusting α, β and γ in the preceding equations. The formula derived by Arnold et al. [24] based on an analysis of the p+Ca experimental data was used as the momentum-dependent potential. The forms of $U_{\rm md}$ and $U_{\rm sym}$ are as follows:

$$U_{\rm md} = \sum_{i,j,j\neq i} t_0 \ln^2\left[1+\varepsilon\left(\vec{p}_i-\vec{p}_j\right)^2\right]\frac{\left\langle\rho(\vec{r},t)\right\rangle_i}{\rho_0}, \quad (6)$$

$$U_{\rm sym} = \frac{C_{\rm sym}}{2\rho_0}\sum_{i,j,j\neq i}\frac{t_{zi}t_{zj}}{(4\pi L)^{\frac{3}{2}}}e^{-\frac{r_{ij}^2}{4L}}. \quad (7)$$

In the preceding equation, $t_0 = 1.58\,\text{MeV}, \varepsilon = 500\,c^2/\text{GeV}^2$ and $C_{\rm sym} = 32$ MeV are the corresponding parameters. The Pauli potential, which is not included in the common IQMD, is introduced to simulate fermions system. The form of the Pauli potential in Ref. [11] is shown as follows:

$$U_{\rm P} = \frac{C_{\rm p}}{2}\left(\frac{\hbar}{q_0 p_0}\right)^3\sum_{i,j,j\neq i}\exp[-\frac{(R_i-R_j)^2}{2q_0^2}-\frac{(P_i-P_j)^2}{2p_0^2}]\delta_{t_i t_j}\delta_{s_i s_j}, \quad (8)$$

where t and s denote the isospin and spin of nucleons, respectively. The values of the potential parameters are $C_{\rm p} = 22$ MeV, $q_0 = 0.46$ fm and $p_0 = 6$ GeV/c, respectively.

2.1 Periodic boundary condition for nuclear matter in IQMD

Periodic boundary conditions are usually used to simulate infinite nuclear matter with a limited number of nucleons. More rigorous periodic boundary conditions are applied to obtain more reasonable results in this work. In previous studies, the periodic boundary condition is generally as described in Ref. [25]. Specifically, a cube with nucleons is surrounded by 26 cubes of the same size and the nucleons in the center cube are subjected to the

interaction of the nucleons in the surrounding 26 cubes. This treatment has been improved in our study. The cubes are not fixed. In calculating the interaction of one nucleon, the center of the center cube will be shifted to this nucleon. Figure 1 is an illustrative explanation of the method, the interaction of the *i*th nucleon and the *j*th nucleon, which is independently related to nucleons in their own cube. To be strictly consistent with this periodic boundary condition, all the potentials and kinetic energy are treated the same way after the evolution of each time step. This means that only the particles in the special cube are considered when calculating these physical quantities for each nucleon.

The introduction of temperature is also an important improvement. As such, we can simulate nuclear matter with different excitations. The Fermi–Dirac distribution is used to describe the momentum distribution of nucleons at temperature T,

$$n(e_k) = \frac{g(e_k)}{e^{\frac{e_k-\mu}{T}}+1}, \tag{9}$$

$$g(e_k) = \frac{V}{2\pi^2}\left(\frac{2m}{\hbar^2}\right)^{\frac{3}{2}}\sqrt{e_k}, \tag{10}$$

where $g(e_k)$ denotes the state-density of the system with kinetic energy e_k. μ_i, the chemical potential, can be obtained by solving the following equation for a fixed temperature [26],

$$\frac{1}{2\pi^2}\left(\frac{2m}{\hbar^2}\right)^{\frac{3}{2}}\int_0^{+\infty}\frac{\sqrt{e_k}}{e^{\frac{e_k-\mu_i}{T}}+1}\mathrm{d}e_k = \rho_i. \tag{11}$$

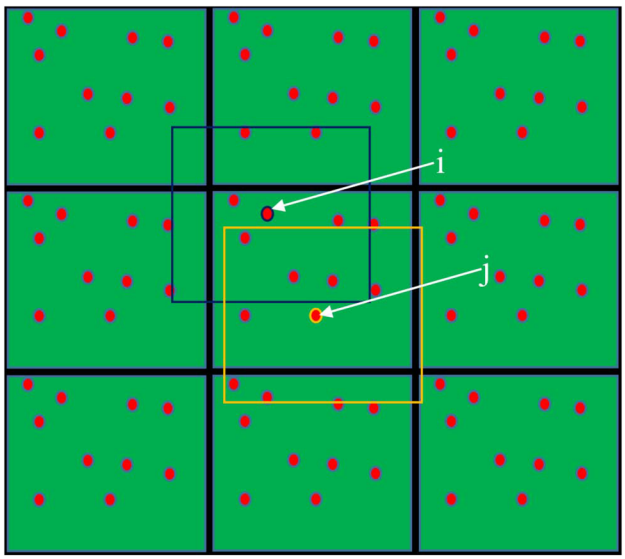

Fig. 1 (Color online) A schematic graph of the periodic boundary condition

2.2 Parameters of effective potentials

Although IQMD is widely used in the simulation of heavy ion collision at intermediate and low energies, the acquired nuclear binding energy has a deviation of 2–3 MeV from the experimental value [27]. Using the periodic boundary condition and the corresponding treatment in the evolution process, we determine that the parameters used for finite nuclei cannot reliably describe the binding energy of nuclear matter. Taking the basic characteristics of infinite nuclear matter into account, as demonstrated in Eq. 12, the two-body, three-body, momentum-dependent, symmetry and Pauli potentials are used to simulate nuclear matter using IQMD.

$$E = \langle E_k\rangle + \left\langle U_{\mathrm{loc}}^{(2)}\right\rangle + \left\langle U_{\mathrm{loc}}^{(3)}\right\rangle + \langle U_{\mathrm{md}}\rangle + \left\langle U_{\mathrm{sym}}\right\rangle + \langle U_{\mathrm{P}}\rangle. \tag{12}$$

As shown in the following equation in IQMD, γ is positively correlated with the incompressibility coefficients of the system above the saturation region.

$$K = 9\rho^2\frac{\partial^2(E/A)}{\partial\rho^2} = \frac{9\beta\gamma(\gamma-1)}{\gamma+1}\left(\frac{\rho}{\rho_0}\right)^{\gamma}. \tag{13}$$

Reasonable values are obtained as illustrated in Table 1. The values are determined separately for each γ by reproducing the binding energy and the requirement of zero pressure for infinite symmetric nuclear matter at the saturation density. We select different γ values corresponding to hard nuclear matter (HM), medium soft nuclear matter (MM) and soft nuclear matter (SM), and the corresponding values of K are 413, 276 and 243. These values are used in subsequent simulations.

3 Results and discussion

3.1 Simulation of nuclear matter

The mass and binding energy are important properties of nuclei [28, 29]. For infinite nuclear matter, the binding energy per nucleon under different conditions is also very important. Using the previously obtained parameters, the binding energies of nuclear matter at different densities and

Table 1 Parameter set of potentials for simulation

	α (MeV)	β (MeV)	γ
HM	− 138.2	68.86	2
MM	− 230.4	160.74	4/3
SM	− 369.51	300.02	7/6

temperatures are simulated in IQMD. In this study, we focus on nuclear matter systems with isospins from $Z/A = 0.1$, 0.2, 0.3, 0.4 and 0.5, which correspond to the asymmetry values (*N*-*Z*)/*A* of 0.8, 0.6, 0.4, 0.2 and 0.0. A total of 1000 nucleons in each cube as well as various temperatures from the ground state (0 MeV) to 10 MeV, with a step size of 2 MeV, are used in the simulations. To accurately represent the effect of density, the densities from 0.25 to 1.75 times the saturation density are determined for each cube in intervals of $0.15\rho_0$. Various densities are determined by changing the edge length of the cube. For example, to obtain nuclear matter at the saturation density, the edge length is approximately 18.0517 fm, for a total of 1000 nucleons.

As shown in Fig. 2, the density dependence of the binding energy for nuclear matter at a fixed temperature is similar to a "∪"-shaped curve with a minimum value near the saturation density. This result is consistent with the general concept that the binding energy is positively correlated with the temperature of the system. The calculations were performed using different parameter sets, including HM, MM and SM. In all these cases, the binding energy at the saturation density point in the ground state is consistent with the theoretical value. The calculation results indicate that with the increase in the incompressibility coefficient, the binding energy curve becomes steeper. This is consistent with theoretical results, because the larger the incompressibility coefficient of nuclear matter, the more rigid it becomes. Due to this property, the binding energy changes more dramatically when the density changes.

The density dependence of the binding energy in the ground state for different isospin asymmetries is shown in Fig. 3. It is evident that the binding energy difference between asymmetry 0.6 and 0.8 is significantly larger than the difference between asymmetries 0 and 0.2. The wave packet width *L* should influence the nuclear properties near to and below the saturation density. However, its effect is diminished for nuclear matter above the saturation density. One of the most basic nuclear properties is that nuclei away from the beta stability line decay easily, and the instability of nuclei is related to the binding energy in that nucleons inside the nucleus with small binding energies are more likely to break through the Coulomb barrier and cause nuclei decay. These results are also consistent with the known stability of nuclei. With the increase in isospin asymmetry, the binding energy becomes positive, which indicates that it is unbound.

3.2 Symmetry energy

Symmetry energy is an important quantity of asymmetric nuclear matter and has an important influence on the

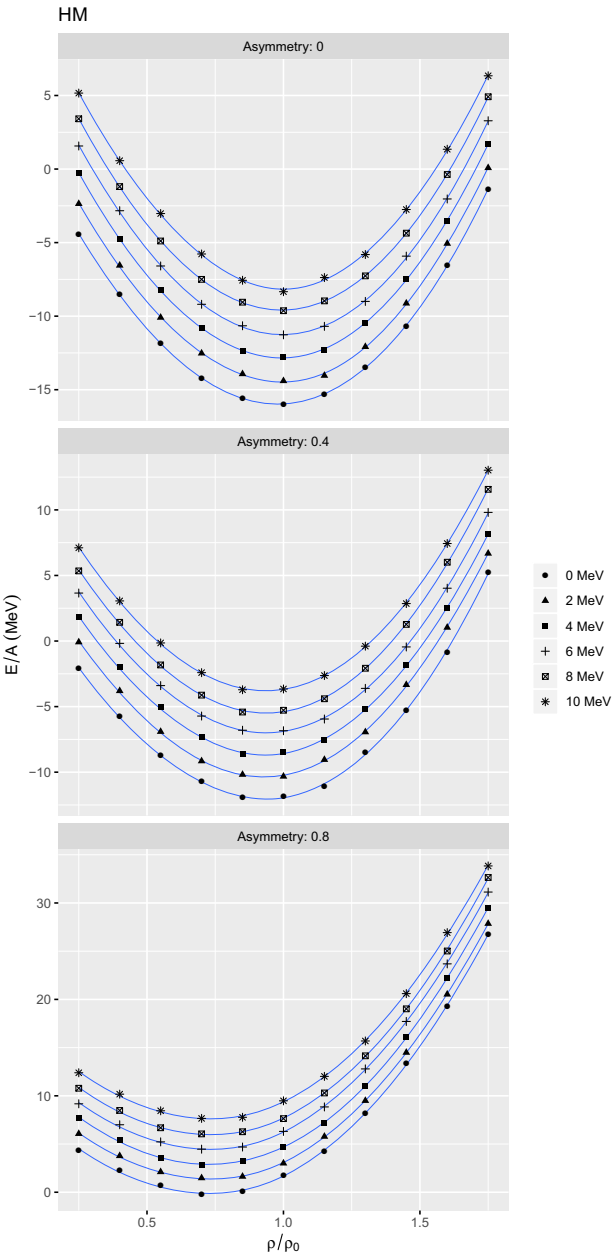

Fig. 2 The density dependence of the binding energy at different temperatures for different isospin asymmetries. The HM parameter set is used in the IQMD calculation

stability of nuclei and the evolution of neutron stars [1, 2]. It has been extensively studied in the recent decades [1–4, 23]. Symmetry energy in medium- and high-energy heavy-ion collisions can be extracted using the QMD model. Usually, the symmetry energy is obtained from theoretical calculations using different models or interaction potentials. In Ref. [23], the symmetry energy is determined based on the density dependence of the binding energy of infinite nuclear matter using molecular dynamics models. In this study, we investigated symmetry energy at

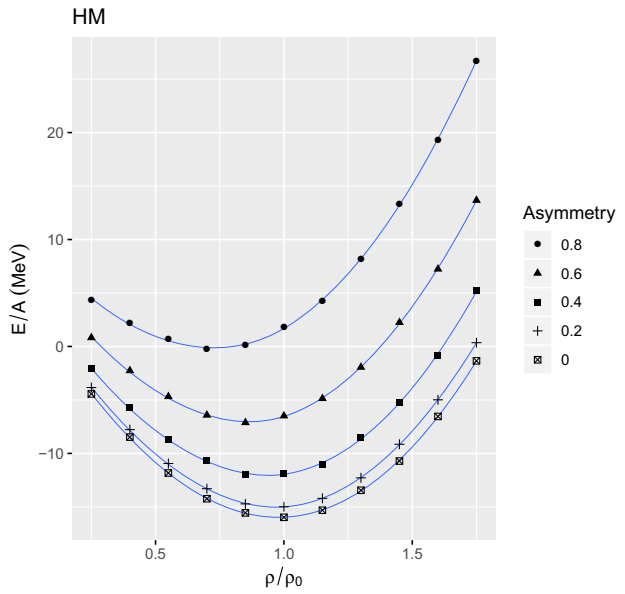

Fig. 3 The density dependence of the binding energy in the ground state for different isospin asymmetries. The HM parameter set is used in the IQMD calculation

different temperatures using the same approach, but within the framework of IQMD.

The binding energy of infinite nuclear matter is dependent on temperature, density and isospin asymmetry. It can be expanded with density as [23],

$$E(T,\rho,\alpha) = E_0(T,\alpha) + E_1(T,\alpha)\rho + E_2(T,\alpha)\rho^2 + E_3(T,\alpha)\rho^3. \tag{14}$$

Given that the power series expression for the binding energy that is expanded based on asymmetry contains only even items, the coefficients in the preceding equation can be expressed as follows:

$$E_0(T,\alpha) = E_{00}(T) + E_{02}(T)\alpha^2 + E_{04}(T)\alpha^4, \tag{15}$$

$$E_1(T,\alpha) = E_{10}(T) + E_{12}(T)\alpha^2 + E_{14}(T)\alpha^4, \tag{16}$$

$$E_2(T,\alpha) = E_{20}(T) + E_{22}(T)\alpha^2 + E_{24}(T)\alpha^4, \tag{17}$$

$$E_3(T,\alpha) = E_{30}(T) + E_{32}(T)\alpha^2 + E_{34}(T)\alpha^4. \tag{18}$$

The nuclear symmetry energy is defined as,

$$E^{\rho}_{\mathrm{sym}} = \frac{\partial^2 E}{2!\partial\alpha^2}. \tag{19}$$

It can then be expressed using the coefficients in the preceding equation,

$$E_{\mathrm{sym}}(T,\rho) = E_{02}(T) + E_{12}(T)\rho + E_{22}(T)\rho^2 + E_{32}(T)\rho^3. \tag{20}$$

These coefficients can be obtained by fitting the binding energy obtained from the simulation data at different densities and isospin asymmetries for a fixed temperature.

The symmetry energy depends on the coefficients of the 2nd power items in the equation for the expanded binding energy expression. The fitting results are listed in Table 2. The differences between CMD and IQMD for nuclear matter calculation can be obtained by comparing the results from IQMD to the various parameter sets (including HM, MM and SM) and the CMD results in Ref. [23].

In Fig. 4, the results at different temperatures ($T = 0, 2, 4, 6, 8, 10$ MeV) that were obtained from IQMD using the HM parameter set are compared with other results. The results at $T = 1, 2, 3, 4, 5$ MeV for CMD are shown. The rhombuses below the reduced density ρ/ρ_0 = 0.2 represent the results obtained from the experiments [30–32]. The dotted line (NL2) and the pentagons around the saturation density are RHF (relativistic Hartree–Fork) calculation results [33]. Theoretical calculations (such as NL2) predict that the symmetry energy is nearly 0 MeV at a very low density. However, the experimental results indicate that it is between 5 MeV and 10 MeV due to the clustering effect at low densities. In this figure, it is evident that both the results obtained for IQMD and CMD are consistent with the experimental results in the low-density region called the liquid–gas mixture region [23]. The non-sensitivity of the quantum or classic model could be due to the small quantum effects in this region. In the high-density region, especially above the saturation density, the results for IQMD are more consistent with the RHF predictions compared to CMD. Moreover, the results for IQMD exhibit a minor difference relative to the RHF calculations. One obvious difference between IQMD and CMD is that there is no quantum effect in the latter. The absence of quantum effects may imply that CMD cannot reliably describe nuclear matter at higher density. However, the potential forms used in CMD and IQMD are different. CMD usually uses relatively simple potentials that lack three-body potential and momentum-dependent potential. These differences between the two models may account for the different results, especially in the higher density region. Further investigations are required to achieve an in-depth understanding.

Table 2 The extracted symmetry energy coefficients for different temperatures

T (MeV)	E_{02}	E_{12}	E_{22}	E_{32}
0	12.327	94.523	− 247.220	898.790
2	9.774	126.153	− 331.481	996.265
4	8.043	142.286	− 237.960	474.658
6	6.725	186.861	− 619.879	1390.171
8	6.559	167.152	− 424.066	957.258
10	7.077	117.178	137.597	− 463.142

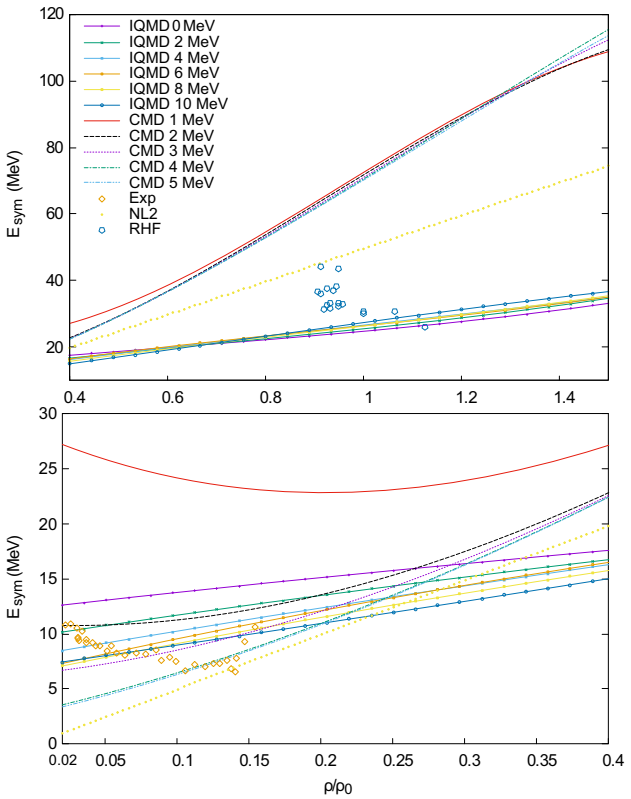

Fig. 4 (Color online) The density dependence of the symmetry energy. For further details, see the main text

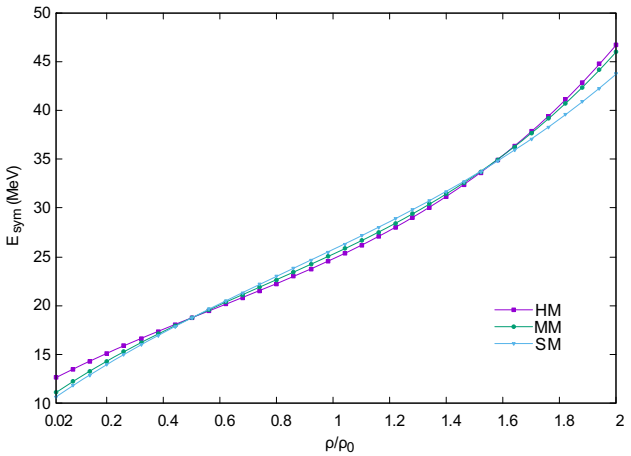

Fig. 5 (Color online) The density dependence of the symmetry energy in the ground state for different potential parameter sets

Figure 5 shows the density dependence of the symmetry energy for nuclear matter in the ground state for IQMD with different potential forms. The results indicate that the parameter sets corresponding to different incompressibility coefficients have a very small effect on the symmetry energy. The symmetry energy near the saturation density is close to 30 MeV, which is confirmed by numerous theoretical calculations. The symmetry energy for different parameter sets exhibits different behaviors above the saturation density (density higher than 1.5 ρ_0) region and for a very low density (below 0.2 ρ_0) region. The symmetry energy with a high incompressibility coefficient becomes larger compared to the case of a low incompressibility coefficient at high density. However, this behavior is reversed in the low-density region.

4 Summary

In this study, an infinite nuclear matter is simulated using the periodic boundary condition within the framework of IQMD. The binding energy of nuclear matter at different densities, isospin asymmetries and temperatures is obtained. By using the same method described in Ref. [23], the symmetry energy can be extracted. The results indicate that IQMD is more suitable for nuclear matter simulation above the saturation density compared to CMD. However, in the low-density region, both models can reliably reproduce the experimental results. The interaction potentials for CMD are relatively simple. This may allow the model to reliably simulate nuclear matter at low density, but the lack of a momentum-dependent potential and a quantum effect suggests that the model cannot reliably describe some characteristics of nuclear matter in the higher density region. This work demonstrates that IQMD may be an adequate model for the study of infinite nuclear matter, but further investigations are required to obtained reliable results.

References

1. M. Baldo, G.F. Burgio, The nuclear symmetry energy. Prog. Part. Nucl. Phys. **91**, 203–258 (2016). https://doi.org/10.1016/j.ppnp.2016.06.006
2. B.A. Li, L.W. Chen, C.M. Ko, Recent progress and new challenges in isospin physics with heavy-ion reactions. Phys. Rep. **464**, 113–281 (2008). https://doi.org/10.1016/j.physrep.2008.04.005
3. P. Danielewicz, J. Lee, Symmetry energy I: semi-infinite matter. Nucl. Phys. A **818**, 36–96 (2009). https://doi.org/10.1016/j.nuclphysa.2008.11.007
4. P. Marini, A. Bonasera, G.A. Souliotis et al., Systematic study of the symmetry energy within the approach of the statistical multifragmentation model. Phys. Rev. C **87**, 024603 (2013). https://doi.org/10.1103/PhysRevC.87.024603
5. N.B. Zhang, B.A. Li, Astrophysical constraints on a parametric equation of state for neutron-rich nucleonic matter. Nucl. Sci. Tech. **29**, 178 (2018). https://doi.org/10.1007/s41365-018-0515-9
6. H. Pais, F. Gulminelli, C. Providencia et al., Light and heavy clusters in warm stellar matter. Nucl. Sci. Tech. **29**, 181 (2018). https://doi.org/10.1007/s41365-018-0518-6

7. J. Aichelin, H. Stocker, Quantum molecular dynamics-a novel approach to n-body correlations in heavy ion collisions. Phys. Lett. B **176**, 14–19 (1986). https://doi.org/10.1016/0370-2693(86)90916-0
8. J. Aichelin, G. Peilert, A. Bohnet et al., Quantum molecular dynamics approach to heavy ion collisions: description of the model, comparison with fragmentation data, and the mechanism of fragment formation. Phys. Rev. C **37**, 2451–2468 (1988). https://doi.org/10.1103/PhysRevC.37.2451
9. J. Aichelin, "Quantum" molecular dynamics—a dynamical microscopic n-body approach to investigate fragment formation and the nuclear equation of state in heavy ion collisions. Phys. Rep. **202**, 233–360 (1991). https://doi.org/10.1016/0370-1573(91)90094-3
10. G. Peilert, J. Randrup, H. Stocker et al., Clustering in nuclear matter at subsaturation densities. Phys. Lett. B **260**, 271–277 (1991). https://doi.org/10.1016/0370-2693(91)91611-X
11. G. Peilert, J. Konopka, H. Stocker et al., Dynamical treatment of fermi motion in a microscopic description of heavy ion collisions. Phys. Rev. C **46**, 1457–1473 (1992). https://doi.org/10.1103/PhysRevC.46.1457
12. Z.Q. Feng, Nuclear dynamics and particle production near threshold energies in heavy-ion collisions. Nucl. Sci. Tech. **29**, 40 (2018). https://doi.org/10.1007/s41365-018-0379-z
13. Z.F. Zhang, D.Q. Fang, Y.G. Ma, Decay modes of highly excited nuclei. Nucl. Sci. Tech. **29**, 78 (2018). https://doi.org/10.1007/s41365-018-0427-8
14. R. Wada, K. Hagel, J. Cibor et al., Entrance channel dynamics in ^{40}Ca + ^{40}Ca at 35a mev, Phys. Lett. B **422**, 6-12 (1998). https://doi.org/10.1016/S0370-2693(98)00033-1
15. T. Maruyama, K. Niita, K. Oyamatsu et al., Quantum molecular dynamics approach to the nuclear matter below the saturation density. Phys. Rev. C **57**, 655–665 (1998). https://doi.org/10.1103/PhysRevC.57.655
16. T. Maruyama, K. Niita, A. Iwamoto, Extension of quantum molecular dynamics and its application to heavy-ion collisions. Phys. Rev. C **53**, 297–304 (1996). https://doi.org/10.1103/PhysRevC.53.297
17. W.B. He, Y.G. Ma, X.G. Cao et al., Giant dipole resonance as a fingerprint of α clustering configurations in ^{12}C and ^{16}O. Phys. Rev. Lett. **113**, 032506 (2014). https://doi.org/10.1103/PhysRevLett.113.032506
18. W.B. He, Y.G. Ma, X.G. Cao et al., Dipole oscillation modes in light α-clustering nuclei. Phys. Rev. C **94**, 014301 (2016). https://doi.org/10.1103/PhysRevC.94.014301
19. S.S. Wang, Y.G. Ma, X.G. Cao et al., Investigation of giant dipole resonances in heavy deformed nuclei with an extended quantum molecular dynamics model. Phys. Rev. C **95**, 054615 (2017). https://doi.org/10.1103/PhysRevC.95.054615
20. W.B. He, X.G. Cao, Y.G. Ma et al., Application of EQMD model to researches of nuclear exotic structures. Nucl. Tech. **37**, 100511 (2014). https://doi.org/10.11889/j.0253-3219.2014.hjs.37.100511. (in Chinese)
21. S.S. Wang, X.G. Cao, T.L. Zhang et al., Study of ground state properties of Nuclei by an extended quantum molecular dynamics model. Nucl. Phys. Rev. **32**, 24 (2015). https://doi.org/10.11804/NuclPhysRev.32.01.024. (in Chinese)
22. J.A. Lopez, E.R. Homs, R. Gonzalez et al., Isospin-asymmetric nuclear matter. Phys. Rev. C **89**, 024611 (2014). https://doi.org/10.1103/PhysRevC.89.024611
23. J.A. Lopez, S.T. Porras, Symmetry energy in the liquid-gas mixture. Nucl. Phys. A **957**, 312–320 (2017). https://doi.org/10.1016/j.nuclphysa.2016.09.012
24. L.G. Arnold, B.C. Clark, E.D. Cooper et al., Energy dependence of the p-^{40}Ca optical potential: a Dirac equation perspective. Phys. Rev. C **25**, 936–940 (1982). https://doi.org/10.1103/PhysRevC.25.936
25. T. Maruyama, K. Niita, K. Oyamatsu et al., Nuclear matter structure studied with quantum molecular dynamics. Nucl. Phys. A **654**, 908c–911c (1999). https://doi.org/10.1016/S0375-9474(00)88570-X
26. D.Q. Fang, Y.G. Ma, C.L. Zhou, Shear viscosity of hot nuclear matter by the mean free path method. Phys. Rev. C **89**, 047601 (2014). https://doi.org/10.1103/PhysRevC.89.047601
27. C. Hartnack, R.K. Puri, J. Aichelin et al., Modelling the many-body dynamics of heavy ion collisions: present status and future perspective. Eur. Phys. J. A **1**, 151–169 (1998). https://doi.org/10.1007/s100500050045
28. D. Benzaid, S. Bentridi, A. Kerraci et al., Bethe-Weizsacker semiempirical mass formula coefficients 2019 update based on AME2016. Nucl. Sci. Tech. **31**, 9 (2020). https://doi.org/10.1007/s41365-019-0718-8
29. D. Wu, C.L. Bai, H. Sagawa et al., Contributions of optimized tensor interactions on the binding energies of nuclei. Nucl. Sci. Tech. **31**, 14 (2020). https://doi.org/10.1007/s41365-020-0727-7
30. S. Kowalski, J.B. Natowitz, S. Shlomo et al., Experimental determination of the symmetry energy of a low density nuclear gas. Phys. Rev. C **75**, 014601 (2007). https://doi.org/10.1103/PhysRevC.75.014601
31. R. Wada, K. Hagel, L. Qin et al., Nuclear matter symmetry energy at $0.03 \leqslant \rho/\rho_0 \leqslant 0.2$. Phys. Rev. C **85**, 064618 (2012). https://doi.org/10.1103/PhysRevC.85.064618
32. K. Hagel, J.B. Natowitz, G. Ropke, The equation of state and symmetry energy of low-density nuclear matter. Eur. Phys. J. A **50**, 39 (2014). https://doi.org/10.1140/epja/i2014-14039-4
33. L.W. Chen, C.M. Ko, B.A. Li, Isospin-dependent properties of asymmetric nuclear matter in relativistic mean field models. Phys. Rev. C **76**, 054316 (2007). https://doi.org/10.1103/PhysRevC.76.054316